

Design, Synthesis, and Evaluation of a Novel Dual Fms-Like Tyrosine Kinase 3/Stem Cell Factor Receptor (FLT3/c-KIT) Inhibitor for the Treatment of Acute Myelogenous Leukemia

Robert J. Davies,^{*,†} Albert C. Pierce,[†] Cornelia Forster,[‡] Ron Grey,[†] Jinwang Xu,[†] Michael Arnost,[†] Deborah Choquette,[§] Vincent Galullo,^{||} Shi-Kai Tian,[⊥] Greg Henkel,[#] Guanqing Chen,[‡] David K. Heidary,[▽] Joanne Ma,[†] Cameron Stuver-Moody,[†] and Mark Namchuk[†]

[†]Vertex Pharmaceuticals Inc., 130 Waverly Street, Cambridge, Massachusetts 02139, United States

[‡]Novartis IBMR, 250 Massachusetts Avenue, Cambridge, Massachusetts 02139, United States

[§]Amgen, 1 Kendall Square, Cambridge, Massachusetts 02139, United States

^{||}Astra Zeneca R&D Boston, 35 Gatehouse Drive, Waltham, Massachusetts 02451, United States

[⊥]University of Science & Technology of China, Hefei, Anhui 230026, China

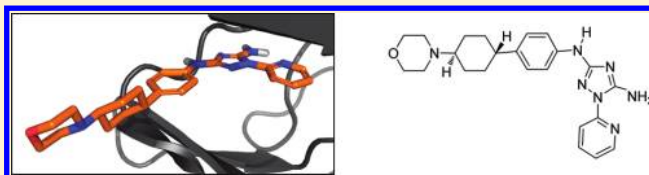
[#]Arisan Therapeutics, 21512 Canaria, Mission Viejo, California 92692, United States

[▽]University of Kentucky, Lexington, Kentucky 40506, United States

^{*}Merck West Point, 770 Sumneytown Pike, West Point, Pennsylvania 19486, United States

 Supporting Information

ABSTRACT: A high-throughput screen of our compound archive revealed a novel class of dual FMS-like tyrosine kinase 3 (FLT3)/c-KIT inhibitors. With the help of molecular modeling, this class was rapidly optimized for both potency against FLT3 and FLT3/c-KIT and excellent potency in cell-based assays, leading to dose-dependent cell death in acute myelogenous leukemia (AML) patient blast samples. Ultimately, the AML patient blast data defined the preferred target profile as we designed and evaluated a set of FLT3 selective and FLT3/c-KIT dual molecules. Further optimization for pharmacokinetic properties resulted in the selection of the dual FLT3/c-KIT inhibitor, *N*³-(4-(*trans*-4-morpholinocyclohexyl)phenyl)-1-(pyridin-2-yl)-1*H*-1,2,4-triazole-3,5-diamine, VX-322 (compound 37), to move forward to preclinical evaluation.



INTRODUCTION

Acute myelogenous leukemia (AML) affects around 30,000 people annually worldwide and represents about 1.2% of cancers diagnosed in the United States.¹ It is the most common adult leukemia and is very aggressive. Over 50% of AML patients are over the age of 60 and are often unable to withstand the high concentrations of cytotoxic agents, AraC and anthracyclines, which are the current standard of care.² The remission rate for this age group is around 50%, and of those, only 10% achieve disease free survival for greater than 5 years.^{3,4} This shows that there is a clear need for better therapeutic agents for this disease.

AML occurs when normal hematopoietic stem cells are mutated into a state where they proliferate in an uncontrolled manner, without differentiating. This causes a dangerous overproduction of leukemic blasts (immature white blood cells) and underproduction of red blood cells and platelets.

AML seems well suited for the therapeutic inhibition of the kinases involved in leukemic cell survival and proliferation. FMS-like tyrosine kinase 3 (FLT3) and stem cell factor

receptor (c-KIT) are two closely related kinases that appear to be good candidates for this inhibition. They are both normally involved in the survival, proliferation, and differentiation of hematopoietic stem cells, but their expression and/or overactivation are common traits of AML blasts.^{5,6}

In AML patient blasts, overexpression of wild-type c-KIT and FLT3 occurs, leading to growth stimulation upon binding of stem cell factor (SCF) or FLT3 ligand (FL).⁷ In over half of these samples, the blasts were found to express both c-KIT and its ligand, SCF, such that the blasts have the potential to stimulate their own proliferation. This blast cell autostimulation also occurs frequently with FLT3 signaling, although through a different mechanism. In the case of FLT3, there are numerous mutations that lead to constitutive activation of the receptor in the absence of ligand. In AML, a number of activating mutations of FLT3 play a pathogenic role through an uncontrolled activation, which leads to a

Received: June 16, 2011

Published: October 04, 2011

rapid proliferation of white blood cells, or blasts, which then interfere with the production of normal blood cells.⁸ The two major activating mutations are an internal tandem duplication (ITD)^{9,10} in the juxtamembrane region and a D835 mutation in the activation loop.¹¹ These mutations are seen in 35% of AML cases and lead to a far worse prognosis for those patients.^{12,13}

AML treatment with small molecule FLT3 inhibitors has been a keen area of research over the past decade and has resulted in several potent compounds progressing to the clinic. Unfortunately, several candidates such as MLN-518 (tandutinib),¹⁴ CEP-701 (lestaurtinib),¹⁵ SU-11248 (sunitinib),¹⁶ and BAY-43-9006 (sorafenib)¹⁷ did not meet the desired end points^{18,19} for a variety of possible reasons, including poor pharmacokinetics, high serum-binding, or poor selectivity. However, PKC-412 (midostaurin)²⁰ is still under development for AML, in addition to one newer, improved FLT3 inhibitor, AC220, which is in midstage AML trials.²¹

The initial aim of our program was to identify potent FLT3 selective compounds, which could be evaluated in vitro and in vivo with the aim of providing a safer, more efficacious treatment for AML. As a first step toward developing such an inhibitor, our compound collection was screened against FLT3.

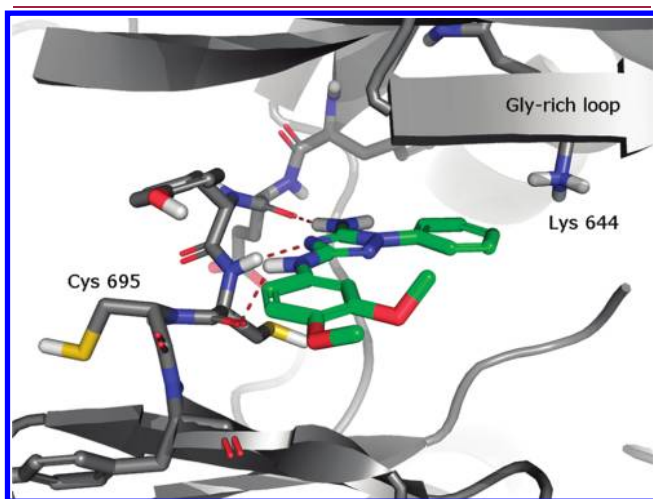
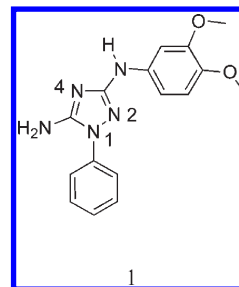


Figure 1. Compound **1** modeled into a FLT3 homology model. Hinge hydrogen bonds are shown as dashed lines.

Compound **1**, a 3,5-diamino-1,2,4-triazole, was one of the most promising hits from this screen, with an inhibition constant against FLT3 of 85 nM and no detectable inhibition of the other kinases tested.

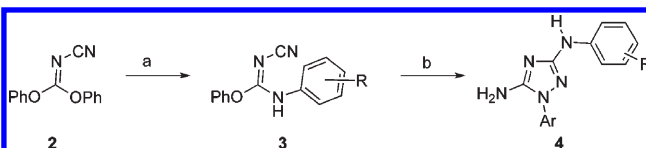


In addition to having a favorable inhibition profile, this hit class could also be readily modeled into the active site of our FLT3 homology model. The binding mode is depicted in Figure 1, with the diaminotriazole moiety making three hydrogen bonds to the hinge. A final advantage of this class was the availability of a facile synthetic route, which allowed for a rapid structure–activity relationship evaluation.

CHEMISTRY

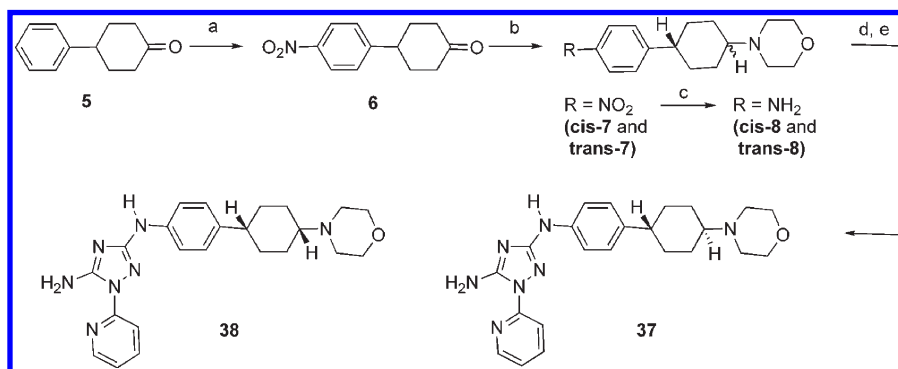
The general synthetic route to the diaminotriazole analogues is depicted in Scheme 1. The triazole is synthesized in a regiospecific manner through the reaction of diphenyl cyanocarbonimidate (**2**) with stepwise displacements of the phenoxy group, first with an appropriately substituted aniline to give the imidate (**3**), followed by cyclization with an aryl hydrazine to give the triazole (**4**). In these cases,

Scheme 1. General Synthetic Route to the 1,2,4-Triazoles^a



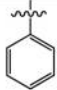
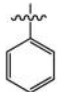

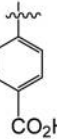
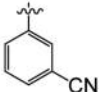
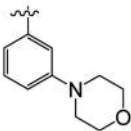

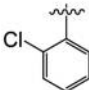
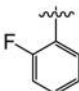
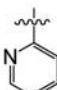
^a Reagents and conditions: (a) ArNH₂, *i*-PrOH or dioxane, reflux. (b) ArNHNH₂, *i*-PrOH, or CH₃CN or DMA, reflux, or microwave 180–220 °C.

Scheme 2. Synthesis of 4-(4-Morpholinocyclohexyl)anilines^a



^a Reagents and conditions: (a) NO₂BF₄, CH₃CN. (b) Morpholine, NaBH(OAc)₃, THF. (c) Zn, NH₄Cl, MeOH, reflux. (d) Compound **2**, *i*PrOH. (e) 2-Pyridylhydrazine, *i*PrOH, MW 180 °C.

Table 1. Effects of Planarity on FLT3 Affinity

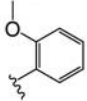
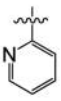
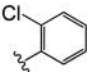
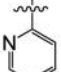
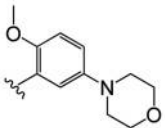
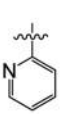
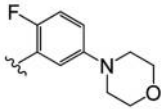
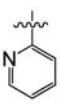
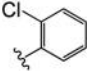
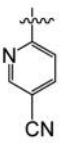
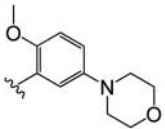
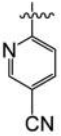
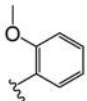
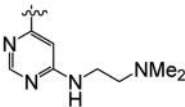
Compound	R1	R2	FLT3 Ki (nM)
1	H		85
9	OMe		42
10	H		22
11	H		24
12	H		210
13	OMe		11
14	OMe		2500
15	H		930
16	H		53
17	H		2.8

the reactions proceed to give predominantly, and in many cases exclusively, the 1,2,4-triazole as reported in the literature.²²

Most of the substituted anilines were commercially available. Key anilines that did require synthesis included the 4-(4-morpholinocyclohexyl)anilines (*cis*- and *trans*-8, Scheme 2). These were prepared through nitration of 4-phenylcyclohexanone (5) using nitronium tetrafluoroborate to give the 4-(4-nitrophenyl)cyclohexanone (6) in 43% yield. Reductive

amination of the cyclohexanone 6 with morpholine gave both a mixture of the *cis* and *trans* isomers of 4-(4-(4-nitrophenyl)cyclohexyl)morpholine (7) in 90% yield, which were separated by flash chromatography with a 1:3 ratio of the *cis*:*trans* products, respectively. Both the *cis*-7 and the *trans*-7 nitro intermediates were reduced to their corresponding anilines (*cis*-8 and *trans*-8). Following the above general procedure (Scheme 1), the triazoles 37 and 38 were obtained.²³

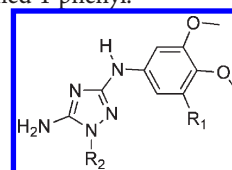
Table 2. Selectivity Effects of Ar1 and Ar2

Compound	Ar1	Ar2	FLT3 Ki (nM)	c-KIT Ki (nM)	Aurora A Ki (nM)	JAK2 Ki(nM)	IRAK4 Ki (nM)
18			15	12	>7000	>4000	420
19			18	ND	2000	>4000	1200
20			6	60	>4000	>4000	160
21			12	37	>3000	590	440
22			15	ND	>2500	>4000	36
23			22	205	2600	>4000	340
24			1	270	2100	>4000	78

RESULTS AND DISCUSSION

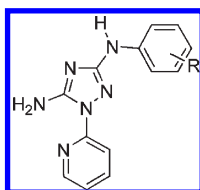
As a selective FLT3 inhibitor, compound **1** provided an excellent starting point for our lead optimization efforts. Compound **9** is included in Table 1 as a second reference compound. Its activity is very similar to **1** but with a slight boost from the introduction of the additional methoxy group. Starting from these reference compounds, the first strategy pursued was to improve FLT3 potency by targeting lysine 644 with the intention of forming an additional hydrogen bond or salt bridge. The homology model in Figure 1 shows that this lysine should be easily reached from the para position of the hydrazine-derived phenyl. The nitrile and carboxyl of compounds **10** and **11** yielded significant potency enhancements, with inhibition constants of 22 and 24 nM, respectively. Compound **12** highlights the importance of the lysine interaction, as the 3-cyano substituent, unable to reach the lysine, leads to a moderate drop-off in potency. This is not to say that 3-substitutions are generally detrimental to activity. This site can access the glycine-rich loop, and hydrophobic groups such as the morpholine of **13** do yield potency improvements. At 11 nM, compound **13** approached the

targeted potency levels but still fell short by approximately 10-fold. Another potency-enhancing strategy attempted was the stabilization of the flat, coplanar conformation of the triazole and the directly attached 1-phenyl.



The phenyl in compounds **1** and **9** is within the adenine-binding portion of the adenosine triphosphate (ATP) site, and compounds mimicking the flat, hydrophobic nature of adenine can be expected to improve potency. To evaluate the benefit of flatness and coplanarity, compounds **14–16** were synthesized, and their potency was assessed. As expected, the cyclohexyl and 2-chlorophenyl groups of **14** and **15** showed substantial loss in potency accompanying their less flat structures. The 2-fluoro of **16** does not have a significant effect relative to the unsubstituted phenyl. The 2-pyridyl analogue

Table 3. Effects of Aniline Variation on in Vitro Kinase Binding, Kinase Selectivity, Cellular Activity, and Rat IV Pharmacokinetics



Compound	Position	R	FLT3 K _i (nM)	c-Kit K _i (nM)	Selectivity ^a	MV-411 IC ₅₀ (nM)	Rat IV-PK	
							Cl (mL/min/kg)	T1/2 (h)
25	para		5	18	147	2	31.1	2.84
26	para		8	NA	130	2	84.4	2.54
27	para		5	38	113	0.9	63.9	1.615
28	para		7	<50	140	1	17.7	1.028
29	para		12	<50	119	NA	67.2	0.93
30	para		11	21	45	2	4.4	2.22
31	meta		10	10	94	NA	16.7	2.923
32	para		12	240	92	18	42.1	1.33
33	meta		9	180	80	15	44.6	2.81
34	para		2	<0.001	366	0.3	77.1	2.446
35	meta		<1	<50	584	<1	174.3	2.481
36	para		5	<50	189	1	25.1	1.419
37	para		2	<1	336	<0.2	9	7.982
38	para		5	ND	147	1	77	1.6

^a Selectivity is calculated as the geometric mean of the K_i values for 13 counterscreened kinases (JNK3, SRC, GSK3, CDK2, KDR, PKA, SYK, JAK2, IRAK4, ROCK1, MET, PLK1, and PI3 kg) divided by the FLT3 K_i.

17 was hypothesized to be the most planar and, therefore, most active, analogue. The internal hydrogen bond to the exocyclic 5-amine locks in the flat conformation without affecting other interactions to the protein, and upon synthesis, this compound had a 2.8 nM inhibition constant.

Although compound 17 is sufficiently potent to determine its efficacy as a FLT3 inhibitor, selectivity remained an issue. Of 13 kinases routinely screened in-house, IRAK4 (43 nM), Janus kinase 2 (JAK2) (67 nM), and Aurora A (103 nM) were inhibited with K_i values at or under 100 nM, as was c-KIT (9 nM), another

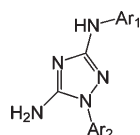
Table 4. Oral PK of Compound 37 in Mouse, Rat, and Monkey

species	dose (mg/kg)	AUC _(0–24 h) (h μ g/mL)	C _{max} (μ g/mL)	T _{max} (h)	T _{1/2} (h)	% F
mouse	20	6.73	0.68	2	15.47	66
rat	30	65.03	5.03	6	8.34	155
monkey	10	12.67	2.55	2.17	3.15	54

Table 5. Characterization of Compound 37 Across a Panel of Primary AML Patient Blast Cells

compd	96-2 (WT)	97-2 (D835Y)	2002-2 (ITD)	2003-3 (WT)	2003-5 (WT)
37	0.1	0.22	0.012	0.02	0.025

kinase involved in hematopoiesis. While we considered the possibility that dual FLT3/c-KIT inhibitors might convey some advantages over selective FLT3 inhibitors, our goal was for a generally selective compound. Because Cys 695 of FLT3 and c-KIT is a proline in Aurora A, JAK2, and IRAK4, it was hypothesized that steric bulk impinging on this residue would be less tolerated in those three kinases than in FLT3, leading to selectivity. To test the hypothesis, a set of analogues was synthesized with 2-substituents on the aniline ring, as shown in Table 2.



The data from these analogues largely confirms our hypothesis, with improved selectivity over Aurora A and JAK2, and modest improvements seen against IRAK4. Unexpectedly, compounds **23** and **24** also showed some degree of selectivity against c-KIT, which allowed us to assess the relative merits of FLT3 selective versus dual FLT3/c-KIT compounds.

A set of FLT3 selective and dual FLT3/c-KIT inhibitors were tested for their ability to induce apoptosis in primary AML patient blast samples. The dual FLT3/c-KIT inhibitors were substantially and consistently more potent than FLT3 selective inhibitors.²⁴ For this reason, the dual FLT3/c-KIT profile became our desired target compound profile and thus dictated our subsequent chemistry endeavors.

In a separate exercise from the 2-substituted aniline analogues described above, a broader aniline substituent exploration was carried out with 2-pyridyl fixed at the 1-position of the triazole. The 3-position offers significant space underneath the flexible glycine-rich loop, while the 4-position sits at the edge of active site with vectors toward solvent. A representative subset of these compounds is shown in Table 3, where it can be seen that a broad range of substituents were tolerated at both positions. This tolerance in potency allowed an extensive search for a compound with optimal potency, selectivity, cell activity, and both physicochemical and pharmacokinetic properties for further preclinical testing. We explored multiple approaches to improve solubility, including a variety of linkers extending basic groups toward solvent. Although we saw improvements in physical properties in cases such as for N-linked compounds such as compound **26**, O-linked compounds such as compound **29** and C-linked compounds such as **34** and **35**, it was not until we extended with a cyclohexyl bridging group that we achieved all of the desired properties in one molecule.

Table 6. Cytotoxicity of Compound 37 against FLT3 and c-KIT Expressing Cell Lines

compd	TF-1 RTK cell panel IC ₅₀ (μ M)				
	FLT3-WT	FLT3-ITD	FLT3 D835Y	c-KIT	TF-1 parental
37	0.0005	0.0013	0.0014	0.0016	>4

Compound **37** met our desired in vitro profile, providing the desired combination of FLT3/c-KIT enzyme potency, subtype selectivity, cellular potency, and good rat IV-PK. The molecule was advanced to multispecies oral PK, which is summarized in Table 4.

Compound **37** showed good oral bioavailability when dosed in 0.5% MC suspension in Balb/c mice, Sprague–Dawley rats, and cynomolgous monkeys. The bioavailability was 66 and 54% in mouse and monkey, respectively, and ranged in the rat between 43 and 155%, which was indicative of good absorption. The half-life following oral dose in rat (at 30 mg/kg) and monkey are similar to the half-life following intravenous dosing in rat and monkey, which is indicative that elimination is not limited by the absorption process at low dose. Importantly, compound **37** was cytotoxic in vitro at low nanomolar concentrations against AML patient isolates²⁵ harboring either wild type or mutant FLT3 (Table 5).

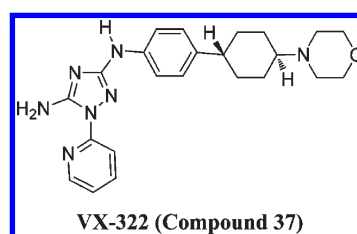
In addition, compound **37** was equally active against AML cell lines expressing FLT3-ITD or c-KIT mutations but was not cytotoxic in the parental cell line (Table 6).

Compound **37** was also efficacious in a FLT3-ITD-dependent myeloproliferative mouse model, doubling survival as compared to other FLT3 inhibitors, with 25% of the mice cured.²⁴ Given these data, compound **37**, a potent dual FLT3/c-KIT inhibitor, was approved for preclinical evaluation.

CONCLUSIONS

From an initial screening hit, the diaminotriazole scaffold was rapidly evolved to produce potent compounds, which could be modified to have either FLT3 selective or selective dual FLT3/c-KIT profiles. The latter dual profile was selected as this proved to be more potent and efficacious against primary AML patient blast cells.

Compound **37** was deemed an ideal candidate, with excellent enzyme and cell potency for both FLT3 and c-KIT, as well as broad selectivity against other protein kinases. The molecule was cytotoxic against both FLT3 and c-KIT expressing cell lines with no effect on cells, which do not express these receptor tyrosine kinases (RTKs).



The molecule also possessed excellent PK across three species, was potent in primary AML patient blast samples, and showed strong efficacy in a Ba/F3-FLT3-ITD leukemia mouse model. On the basis of these findings, compound **37** was selected to move forward toward preclinical evaluation.

EXPERIMENTAL SECTION

All commercially available reagents and anhydrous solvents were used without further purification. Purity assessment for final compounds based on analytical HPLC: column, 4.6 mm \times 50 mm Waters YMC Pro-C18 column, 5 μ m, 120A. Mobile phases are as follows: A, H₂O with 0.2% formic acid; B, acetonitrile with 0.2% formic acid; gradient, 10–90% B in 3 min with 5 min run time. The flow rate is 1.5 mL/min. Unless specified otherwise, all compounds were \geq 95% purity. Mass samples were analyzed on a Micro Mass ZQ ZMD, Quattro LC, or Quattro II mass spectrometer operated in a single MS mode with electrospray ionization. Samples were introduced into the mass spectrometer using flow injection (FIA) or chromatography. The mobile phase for all mass analysis consisted of acetonitrile–water mixtures with either 0.2% formic acid or ammonium formate. The high-resolution mass spectrum was measured using a 9.4T APEX III FTMS Bruker Daltonics instrument. ¹H NMR spectra were recorded either using a Bruker DRX-500 (500 MHz) or a Bruker Avance II-300 (300 MHz) instrument. The column chromatography was performed using Merck silica gel 60 (0.040–0.063 mm). Preparative reversed phase chromatography was carried out using a Gilson 215 liquid handler coupled to a UV–vis 156 Gilson detector, an Agilent Zorbax SB-C18 column, 21.2 mm \times 100 mm, a linear gradient from 10–90% CH₃CN in H₂O over 10 min (0.1% trifluoroacetic acid); the flow rate was 20 mL/min. Most of the anilines and the hydrazines were commercially available or synthesized following literature procedures.

4-(4-Nitrophenyl)cyclohexanone (6). To a solution of 4-phenylcyclohexanone (4.36 g, 25 mmol) in dry acetonitrile (200 mL) cooled with an acetone–dry ice bath was added nitronium tetrafluoroborate (4.68 g, 35 mmol) in one portion under N₂. After it was stirred for 15 min, the reaction mixture was stirred at 0 °C for 2 h, treated with ice chips, and evaporated. The residue was suspended in water and extracted with ethyl acetate (EtOAc) (3 \times), and the organic phase was washed with brine, dried (Na₂SO₄), filtered, and evaporated. The residue was purified by flash chromatography (SiO₂) eluted with EtOAc/hexanes (15:85) to give 4-(2-nitrophenyl)cyclohexanone (475 mg, yellow solid, 8.6% yield) and then the desired product 4-(4-nitrophenyl)cyclohexanone **6** (2.36 g, yellow solid, 43% yield). FIA-MS: 220.1 [M + 1]. ¹H NMR (500 MHz, CDCl₃): δ 8.12 (dt, *J* = 8.7, 2.2, 2H), 7.34 (dt, *J* = 8.7, 2.2, 2H), 3.08 (tt, *J* = 12.2, 3.4 Hz, 1H), 2.51–2.43 (m, 4H), 2.18 (ddd, *J* = 10.5, 5.8, 3.2 Hz, 2H), 1.97–1.83 (m, 2H).

4-(cis-4-(4-Nitrophenyl)cyclohexyl)morpholine (cis-7) and 4-(trans-4-(4-Nitrophenyl)cyclohexyl)morpholine (trans-7). A suspension of 4-(4-nitrophenyl)cyclohexanone **6** (493 mg, 2.28 mmol), morpholine (0.2 mL, 2.28 mmol), and sodium triacetoxyborohydride (678 mg, 3.2 mmol) in THF (15 mL) was stirred for 24 h. Thin-layer chromatography (TLC) indicated that the reaction was incomplete. Additional sodium triacetoxyborohydride (151 mg) was added. The reaction mixture was stirred for another 24 h, treated with saturated sodium bicarbonate, and extracted with EtOAc (3 \times). The combined organic phases were washed with brine, dried over anhydrous Na₂SO₄, filtered, and evaporated. The crude was purified by flash chromatography (SiO₂) eluted with dichloromethane (CH₂Cl₂)/methanol (MeOH)/28% ammonium hydroxide (NH₄OH) (98:2:0.2) to give *cis*-7 as a yellow oil (428 mg, 65% yield) and *trans*-7 as a yellow solid (150 mg, 23%). Data for *cis*-7: FIA-MA: 291.1 [M + 1]. ¹H NMR (500 MHz, DMSO-*d*₆): δ 8.16 (d, *J* = 8.9 Hz, 2H), 7.52 (d, *J* = 8.8 Hz, 2H), 3.62 (t, *J* = 4.6 Hz, 4H), 2.82 (tt, *J* = 10.9, 3.7 Hz, 1H), 2.39 (br.s, 4H), 2.18 (s, 1H),

2.02–1.89 (m, 2H), 1.82 (dt, *J* = 13.1, 11.1 Hz, 2H), 1.59–1.47 (m, 4H). Data for *trans*-7: FIA-MS: 291.1 [M + 1]. ¹H NMR (500 MHz, DMSO-*d*₆): δ 8.14 (d, *J* = 8.7 Hz, 2H), 7.52 (d, *J* = 8.7 Hz, 2H), 3.60–3.54 (m, 4H), 2.63 (tt, *J* = 11.9, 3.3 Hz, 1H), 2.6 (m, 4H), 2.30 (m, 1H), 1.93 (d, *J* = 11.5 Hz, 2H), 1.88 (d, *J* = 11.9 Hz, 2H), 1.51 (q, *J* = 13.6 Hz, 2H), 1.36 (q, *J* = 12.6 Hz, 2H).

4-(trans-4-Morpholinocyclohexyl)aniline (trans-8) and N³-(4-(trans-4-Morpholinocyclohexyl)phenyl)-1-(pyridin-2-yl)-1H-1,2,4-triazole-3,5-diamine (37). To a solution of 4-(trans-4-morpholinocyclohexyl)morpholine (150 mg, 0.52 mmol) in MeOH (15 mL) were added zinc dust (169 mg, 2.58 mmol) and ammonium chloride (110 mg, 2.0 mmol). The resulting suspension was heated under reflux for 1 h, cooled to room temperature, filtered through Celite, and washed with MeOH. The filtrate was evaporated to give crude 4-(trans-4-morpholinocyclohexyl)aniline (*trans*-8). LC-MS: 261.1 [M + 1]. Without further purification, the aniline was dissolved in isopropanol (20 mL) and stirred with diphenyl cyanocarbonylimide (129 mg, 0.54 mmol) for 5 days under N₂. The solvent was removed in vacuo, and the residue was purified by flash chromatography (SiO₂) (CH₂Cl₂/MeOH/28% NH₄OH 96:4:0.4) to give phenyl *N'*-cyano-*N*-(4-(trans-4-morpholinocyclohexyl)phenyl)-carbonylimide as an off-white solid (113 mg, 57% yield). FIA-MS: 405.1 [M + 1], 403.2 [M – 1]. ¹H NMR (500 MHz, DMSO-*d*₆): δ 10.6 (s, 1H, NH), 7.44 (t, *J* = 7.8 Hz, 2H), 7.35 (d, *J* = 8.3 Hz, 2H), 7.32–7.21 (m, 5H), 3.57 (m, 4H), 2.47 (m, 1H), 2.7–2.5 (m, 5H), 2.31–2.23 (m, 1H), 1.92 (d, *J* = 10.0 Hz, 2H), 1.84 (d, *J* = 11.7 Hz, 2H), 1.45 (q, *J* = 13.7 Hz, 2H), 1.33 (q, *J* = 13.7 Hz, 2H).

A mixture of phenyl *N'*-cyano-*N*-(4-(trans-4-morpholinocyclohexyl)phenyl)carbonylimide (113 mg, 0.28 mmol) and 2-pyridylhydrazine (32 mg, 0.29 mmol) in isopropanol (3 mL) was heated in a microwave oven at 180 °C for 10 min. After the mixture was cooled, the precipitate was collected and washed with isopropanol to give 61 mg of *N*³-(4-(trans-4-morpholinocyclohexyl)phenyl)-1-(pyridin-2-yl)-1H-1,2,4-triazole-3,5-diamine (**37**). The product was further purified by reverse phase HPLC (C-18, water/CH₃CN). LC-MS: 420.1 [M + 1]. ¹H NMR (500 MHz, DMSO-*d*₆): δ 9.59 (br. s, 1H), 8.99 (s, 1H), 8.41 (d, *J* = 4.4 Hz, 1H), 7.97 (t, *J* = 7.8 Hz, 1H), 7.68 (d, *J* = 8.3 Hz, 1H), 7.65 (br. s, 1H), 7.54 (d, *J* = 8.5 Hz, 2H), 7.21 (dd, *J* = 7.2, 5.5, 1H), 7.11 (d, *J* = 8.4 Hz, 2H), 4.02 (d, *J* = 11.3 Hz, 2H), 3.70 (t, *J* = 11.9 Hz, 2H), 3.44 (d, *J* = 11.8 Hz, 2H), 3.28 (m, 1H), 3.20–3.09 (m, 2H), 2.45 (t, *J* = 11.6 Hz, 1H), 2.18 (d, *J* = 11.8 Hz, 2H), 1.96 (d, *J* = 12.5 Hz, 2H), 1.58 (q, *J* = 11.7 Hz, 2H), 1.49 (q, *J* = 12.7 Hz, 2H).

4-(cis-4-Morpholinocyclohexyl)aniline (cis-5') and N³-(4-(cis-4-Morpholinocyclohexyl)phenyl)-1-(pyridin-2-yl)-1H-1,2,4-triazole-3,5-diamine (38). As described for *trans*-8, with 4-(cis-4-morpholinocyclohexyl)morpholine (428 mg, 1.47 mmol), zinc dust (482 mg, 7.37 mmol) and ammonium chloride (316 mg, 5.90 mmol) in MeOH (15 mL) gave *cis*-5'. After treatment with diphenyl cyanocarbonylimide (369 mg, 1.55 mmol) in isopropanol (20 mL), phenyl *N'*-cyano-*N*-(4-(cis-4-morpholinocyclohexyl)phenyl)carbonylimide was obtained as a yellow solid (328 mg, 55% yield). LC-MS: 404.2 [M + 1]. ¹H NMR (500 MHz, DMSO-*d*₆): δ 10.7 (s, 1H), 7.44 (t, *J* = 7.9 Hz, 2H), 7.37 (d, *J* = 8.5 Hz, 2H), 7.33–7.22 (m, 5H), 3.61 (m, 4H), 2.67–2.61 (m, 1H), 2.39 (br. s, 4H), 2.17 (br. s, 1H), 1.96–1.90 (m, 2H), 1.86–1.69 (m, 2H), 1.55–1.42 (m, 4H).

As described for **37**, with phenyl *N'*-cyano-*N*-(4-(cis-4-morpholinocyclohexyl)phenyl)carbonylimide (328 mg, 0.81 mmol), 2-pyridylhydrazine (92 mg, 0.85 mmol) in isopropanol (3 mL) to give 134 mg of **38** after reverse phase HPLC purification. LC-MS: 420.1 [M + 1]. ¹H NMR (500 MHz, DMSO-*d*₆): δ 9.21 (br. s, 1H), 9.01 (s, 1H), 8.41 (d, *J* = 3.2 Hz, 1H), 7.98 (td, *J* = 7.85, 1.86, 1H), 7.68 (d, *J* = 8.4 Hz, 1H), 7.65 (s, 1H), 7.59 (d, *J* = 8.6 Hz, 2H), 7.23 (d, *J* = 8.6 Hz, 2H), 7.22–7.17 (m, 1H), 3.97 (d, *J* = 10.9 Hz, 2H), 3.68 (t, *J* = 11.8 Hz, 2H), 3.49 (d, *J* = 12.2 Hz, 2H), 3.32 (br. s, 1H), 3.04 (q, *J* = 11.3 Hz, 2H), 2.85 (br. s, 1H), 2.18–2.06 (m, 2H), 1.92–1.85 (m, 2H), 1.79–1.70 (m, 4H).

Biochemical Kinase Assays. The kinase activity against FLT3 or c-KIT was determined by radiometric assays using a recombinant human FLT3 or c-KIT kinase domain. The assay was carried out in 96-well plates containing 100 mM 4-(2-hydroxyethyl)-1-piperazineethanesulfonic acid (HEPES) (pH 7.5), 10 mM MgCl₂, 25 mM NaCl, 0.01% bovine serum albumin (BSA), 1 mM dithiothreitol (DTT), 0.5 mg/mL polyE4Y, with 1.5 nM FLT3 or 5 nM c-KIT, and ³³P ATP at 90 and 700 μM, respectively. Inhibitors were dissolved in DMSO, and the reaction was initiated by the addition of ³³P ATP and polyE4Y. After 20 min, the reaction was quenched with 50 μL of 20% TCA containing 4 mM ATP. The reaction mix was transferred to GF/B filter plates and washed three times with 5% TCA. Following the addition of 50 μL of Ultimate Gold scintillant, the samples were counted in a Packard TopCount. The K_i value was determined by fitting the data to the kinetic model for competitive tight binding inhibition. Kinase selectivity assays were performed either at Vertex using a spectrophotometric readout or were performed at Millipore (Billerica, MA) using their KinaseProfiler protocols.

Molecular Modeling. Almost all molecular modeling was performed with a homology model of FLT3 based on the original crystal structure of Vascular Endothelial Growth Factor Receptor 2 (KDR; PDB code 1VR2).²⁶ Late in the course of this work, the FLT3 crystal structure became available (PDB code 1RJB) for use in modeling.²⁷ In using the FLT3 structure for modeling, the JM-B domain of the juxtamembrane domain was removed from the active site to accommodate ligand binding. The KDR-based homology was generated with the MOE software package, and all ligands were built and evaluated in MOE using the MMFF94x force field.²⁸

■ ASSOCIATED CONTENT

S Supporting Information. ¹H NMR and MS spectral data for all of the final compounds. This material is available free of charge via the Internet at <http://pubs.acs.org>.

■ AUTHOR INFORMATION

Corresponding Author

*Tel: 617-444-6506. E-mail: robert_davies@vrtx.com.

■ ABBREVIATIONS USED

FLT3, FMS-like tyrosine kinase 3; AML, acute myelogenous leukemia; RTK, receptor tyrosine kinase; ITD, internal tandem duplication; JAK2, Janus kinase 2; TLC, thin-layer chromatography; MeOH, methanol; EtOAc, ethyl acetate; CH₂Cl₂, dichloromethane; NH₄OH, ammonium hydroxide; HEPES, 4-(2-hydroxyethyl)-1-piperazineethanesulfonic acid; DTT, dithiothreitol; ATP, adenosine triphosphate; BSA, bovine serum albumin

■ REFERENCES

- (1) Groves, F. D.; Linet, M. S.; Devesa, S. S. Patterns of occurrence of the leukemias. *Eur. J. Cancer* **1995**, *31A*, 941–949.
- (2) Appelbaum, F. R.; Gundacker, H.; Head, D. R.; Slovak, M. L.; Willman, C. L.; Godwin, J. E.; Anderson, J. E.; Petersdorf, S. H. Age and acute myeloid leukemia. *Blood* **2006**, *107*, 3481–3485.
- (3) Kantarjian, H.; O'Brien, S.; Cortes, J.; Giles, F.; Faderl, S.; Jabbour, E.; Garcia-Manero, G.; Wierda, W.; Pierce, S.; Shan, J.; Estey, E. Results of intensive chemotherapy in 998 patients age 65 years or older with acute myeloid leukemia or high-risk myelodysplastic syndrome: Predictive prognostic models for outcome. *Cancer* **2006**, *106*, 1090–1098.

- (4) Tallman, M. S. New strategies for the treatment of acute myeloid leukemia including antibodies and other novel agents. *Hematol. Am. Soc. Hematol. Educ. Program* **2005**, 143–150.
- (5) Kell, J. Emerging treatments in acute myeloid leukaemia. *Expert Opin. Emerging Drugs* **2004**, *9*, 55–71.
- (6) Banerji, L.; Sattler, M. Targeting mutated tyrosine kinases in the therapy of myeloid leukaemias. *Expert Opin. Ther. Targets* **2004**, *8*, 221–239.
- (7) Stacchini, A.; Fubini, L.; Severino, A.; Sanavio, F.; Aglietta, M.; Piacibello, W. Expression of type III receptor tyrosine kinases FLT3 and KIT and responses to their ligands by acute myeloid leukemia blasts. *Leukemia* **1996**, *10* (10), 1584–1591.
- (8) Kiyoi, H.; Naoe, T. FLT3 mutations in acute myeloid leukemia. *Methods Mol. Med.* **2006**, *125*, 189–197.
- (9) Nakao, M.; Yokota, S.; Iwai, T.; Kaneko, H.; Horiike, S.; Kashima, K.; Sonoda, Y.; Fujimoto, T.; Misawa, S. Internal tandem duplication of the *flt3* gene found in acute myeloid leukemia. *Leukemia* **1996**, *10* (12), 1911–1918.
- (10) Quentmeier, H.; Reinhardt, J.; Zaborski, M.; Drexler, H. G. FLT3 mutations in acute myeloid leukemia cell lines. *Leukemia* **2003**, *17*, 120–124.
- (11) Yamamoto, Y.; Kiyoi, H.; Nakano, Y.; Suzuki, R.; Koda, Y.; Miyawaki, S.; Asou, N.; Kuriyama, K.; Yagasaki, F.; Shimazaki, C.; Akiyama, H.; Saito, K.; Nishimura, M.; Motoji, T.; Shinagawa, K.; Takeshita, A.; Saito, H.; Ueda, R.; Ohno, R.; Naoe, T. Activating mutation of D835 within the activation loop of FLT3 in human hematologic malignancies. *Blood* **2001**, *97*, 2434–2439.
- (12) Beran, M.; Luthra, R.; Kantarjian, H.; Estey, E. FLT3 mutation and response to intensive chemotherapy in young adult and elderly patients with normal karyotype. *Leuk. Res.* **2004**, *28*, 547–550.
- (13) Kottaridis, P. D.; Gale, R. E.; Linch, D. C. Prognostic implications of the presence of FLT3 mutations in patients with acute myeloid leukemia. *Leuk. Lymphoma* **2003**, *44*, 905–913.
- (14) Cheng, Y.; Paz, K. Tandutinib, an oral, small-molecule inhibitor of FLT3 for the treatment of AML and other cancer indications. *IDrugs* **2008**, *11* (1), 46–56.
- (15) Levis, M.; Tse, K. F.; Zheng, R.; Baldwin, B. R.; Smith, B. D.; Jones-Brolin, S.; Ruggeri, B.; Dionne, C.; Small, D. A. FLT3-targeted tyrosine kinase inhibitor is cytotoxic to leukemia cells in vitro and in vivo. *Blood* **2002**, *99* (11), 3885–3891.
- (16) O'Farrell, A. M.; Abrams, T. J.; Yuen, H. A.; Ngai, T. J.; Louie, S. G.; Yee, K. W. H.; Wong, L. M.; Hong, W.; Lee, L. B.; Town, A.; Smolich, B. D.; Manning, W. C.; Murray, L. J.; Heinrich, M. C.; Cherrington, J. M. SU11248 is a novel FLT3 tyrosine kinase with potent activity in vitro and in vivo. *Blood* **2003**, *101* (9), 3597–3605.
- (17) Mori, S.; Cortes, J.; Kantarjian, H.; Zhang, W.; Andreeff, M.; Ravandi, F. Potential role of sorafenib in the treatment of acute myeloid leukemia. *Leuk. Lymphoma* **2008**, *49* (12), 2246–2255.
- (18) Kindler, T.; Lipka, D. B.; Fischer, T. FLT3 as a therapeutic target: still challenging after all these years. *Blood* **2010**, *116* (24), 5089–5102.
- (19) Pratz, K. W.; Cortes, J.; Roboz, G. J.; Rao, N.; Arowojolu, O.; Stine, A.; Shiotsu, Y.; Shudo, A.; Akinaga, S.; Small, D.; Karp, J. E.; Levis, M. A pharmacodynamic study of the FLT3 inhibitor KW-2449 yields insight into the basis for clinical response. *Blood* **2009**, *113*, 3938–3946.
- (20) Stone, R. M.; DeAngelo, D. J.; Klimek, V.; Galinsky, I.; Estey, E.; Nimer, S. D.; Grandin, W.; Lebowitz, D.; Wang, Y.; Cohen, P.; Fox, E. A.; Neuberg, D.; Clark, J.; Gilliland, D. G.; Griffin, J. D. Patients with acute myeloid leukemia and an activating mutation in FLT3 respond to a small-molecule FLT3 tyrosine kinase inhibitor, PKC412. *Blood* **2005**, *105* (1), 54–60.
- (21) Zarrinkar, P. P.; Gunawardane, R. N.; Cramer, M. D.; Gardner, M. F.; Brigham, D.; Belli, B.; Karaman, M. W.; Pratz, K. W.; Pallares, G.; Chao, Q.; Sprinkle, K. G.; Patel, H. K.; Levis, M.; Armstrong, R. C.; James, J.; Bhagwat, S. S. AC220 is a uniquely potent and selective inhibitor of FLT3 for the treatment of acute myeloid leukemia (AML). *Blood* **2009**, *114* (14), 2984–2992.

(22) Dunstan, A. R.; Weber, H. P.; Rihs, G.; Widmer, H.; Dziadulewicz, E. K. Concise and regiospecific syntheses of tri-substituted 1,2,4-triazoles. *Tetrahedron Lett.* **1998**, *39*, 7983–7986.

(23) Davies, R. J.; Forster, C. J.; Arnost, M. J.; Wang, J. Triazoles useful as inhibitors of protein kinases and their preparation, pharmaceutical compositions, and use for treatment of various disorders, WO 2006047256 A1 20060504.

(24) Heidary, D. K.; Huang, G.; Ma, J.; Boucher, D.; Forster, C.; Grey, R.; Xu, J.; Chen, G.; Zhou, J.; Namchuk, M.; Yao, M.; Stack, J.; Ball, E. D.; Davies, R. J.; Henkel, G. VX-322: A Novel Dual Receptor Tyrosine Kinase Inhibitor for the Treatment of AML. *J. Med. Chem.* **2011**.

(25) Primary leukemic blasts isolated from peripheral blood of AML patients were characterized for FLT3 mutations by RT-PCR and for cell-surface expression of FLT3, KIT, and the hematopoietic precursor marker CD34 by flow cytometry. FLT3 and KIT-positive blasts from four patients were incubated for 72 h with compound in the presence of human serum, FL, SCF, and GM-CSF, and then, viability was measured by ATP-luciferase assay.

(26) McTigue, M. A.; Wickersham, J. A.; Pinko, C.; Showalter, R. E.; Parast, C. V.; Tempczyk-Russell, A.; Gehring, M. R.; Mroczkowski, B.; Kan, C.-C.; Villafranca, J. E.; Appelt, K. Crystal structure of the kinase domain of human vascular endothelial growth factor receptor 2: A key enzyme in angiogenesis. *Structure* **1999**, *3*, 319–330.

(27) Griffith, J.; Black, J.; Faerman, C.; Swenson, L.; Wynn, M.; Lu, F.; Lippke, J.; Saxena, K. The Structural Basis for Autoinhibition of FLT3 by the Juxtamembrane Domain. *Mol. Cell* **2004**, *13*, 169–178.

(28) *Molecular Operating Environment* (MOE, version 2002.03); Chemical Computing Group: Montreal, PQ, Canada, 2002.